Contents lists available at ScienceDirect

Petroleum Science

journal homepage: www.keaipublishing.com/en/journals/petroleum-science



Original Paper

Study of the liquid resistance effect of water-in-oil emulsions in porous media



Lei-Lei Jia ^a, Li-Guo Zhong ^{a, *}, Shi-Hao Li ^a, Yu-Hao Liu ^a, Chang-Hao Hu ^b, Guo-Dong Wang ^b, Yu-Ning Gong ^b, Ce Shang ^b, Xiao-Cheng Zhang ^c, Yao-Tu Han ^c, Jin Li ^c

- ^a Unconventional Petroleum Research Institute, China University of Petroleum (Beijing), Beijing, 102249, China
- ^b Exploration and Development Research Institution, Liaohe Oilfield of China National Petroleum Corp, Panjin, 124099, Liaoning, China
- ^c State Key Laboratory of Offshore Oil Exploitation, China National Offshore Oil Corporation—Tianjin, Tianjin, 300459, China

ARTICLE INFO

Article history: Received 2 January 2024 Received in revised form 18 July 2024 Accepted 18 July 2024 Available online 19 July 2024

Edited by Yan-Hua Sun

Keywords: Offshore oilfield Crude oil emulsification **Emulsion stability** Liquid resistance effect Seepage resistance

ABSTRACT

During heavy oil recovery in the Bohai Oilfield, substantial emulsification of oil and water occurred. primarily forming water-in-oil emulsions. This phenomenon could alter fluid dynamics within the subsurface porous media, potentially impacting well production performance. To elucidate the properties of water-in-oil emulsions and their associated liquid resistance effects, this study conducted a series of rheological tests, microscopic examinations, and injection experiments. The results show that the droplet size and distribution of water-in-oil emulsions were primarily influenced by shear rate and water content, which in turn modified emulsion viscosity. The stability of water-in-oil emulsions was reduced when they flowed through porous media. The increase in emulsion viscosity and the liquid resistance effect collectively enhanced the seepage resistance of water-in-oil emulsions flowing through porous media. Notably, when the emulsion droplet size exceeded the pore throat size, over 90% of the total seepage resistance was attributable to the liquid resistance effect. Conversely, when the majority of the emulsion droplets were smaller than the pore throat, the viscosity accounted for more than 60% of the seepage resistance. Water-in-oil emulsions flowed through cores with permeabilities ranging from 50 to 100 mD, exhibiting threshold pressure gradients between 35 and 43 MPa/m. At a core permeability of 300 mD, the threshold pressure gradient was significantly reduced to 1 MPa/m. The presence of a waterin-oil emulsion in the reservoir could result in a production pressure differential falling below the threshold pressure, thereby reducing reservoir productivity.

© 2024 The Authors. Publishing services by Elsevier B.V. on behalf of KeAi Communications Co. Ltd. This is an open access article under the CC BY-NC-ND license (http://creativecommons.org/licenses/by-nc-nd/ 4.0/).

1. Introduction

Offshore oilfields in China possess substantial oil and gas resources, contributing significantly to energy security concerns (Xue, 2018; Wang and Xia, 2009). Currently, offshore oilfields are exploited through pre-drilling: wells are drilled, shut in, and left to soak for 2-4 months before being put into production after the installation of conduit racks. Field data indicate that the oil wells were put into production after 2-4 months of shut-in, the production pressure differential was higher, mainly in the range of 4.1-8.1 MPa, and daily oil production was in the range of 6-64 m³/ d. The oil wells were put into production directly after well

completion; the production pressure differential was lower, mainly in the range of 0.18-3.05 MPa; and daily oil production was in the range of 107–264 m³/d. The production capacity of wells was generally decreased following soaking after pre-drilling. The oil field faces considerable challenges, including significant variations in well production capacity and crude oil emulsification. A key scientific issue in this oil field is that the characteristics of crude oil emulsification in porous media are unclear.

Crude oil emulsification is traditionally characterized by parameters such as emulsion viscosity, droplet size, and stability. Changes in emulsion viscosity under different conditions are commonly represented by viscosity-temperature curves or variable shear rate curves (Onaizi, 2022; Pu et al., 2022; Cao et al., 2022). When examining the size of an emulsion droplet, methods such as mathematical analysis and microscopic scrutiny are frequently employed to clarify the range of droplet sizes in

E-mail address: zhongliguo@cup.edu.cn (L.-G. Zhong).

^{*} Corresponding author.

emulsions. While this approach effectively correlates emulsion droplet size with water content, it provides limited insights into the intricate interactions between emulsion viscosity, droplet size, water content, and the underlying mechanisms (Liu et al., 2022a, 2023b; Gu et al., 2022; Chen et al., 2023). Various techniques, such as stirring, ultrasonic vibration, and the crude oil and water phases flowing through the porous media, are employed in emulsification processes (Adil and Onaizi, 2022; Li et al., 2023; Sun et al., 2022). Previous studies have explored the factors affecting emulsion stability, indicating that higher temperatures increase molecular thermal motion, thereby accelerating the separation of emulsions. Furthermore, increased water content promotes the aggregation of small water droplets, which in turn reduces emulsion stability (Dong et al., 2022; Vladisavljević, 2015). Enhanced shear rates result in the dispersion of water droplets into smaller droplets, increasing the free energy of the system and thereby enhancing emulsion stability (Patil et al., 2021; Ma et al., 2022). The emulsion stability was evaluated by monitoring the time required for the emulsion to break up into its separate phases (Gong et al., 2022; Abdullah and Al-Lohedan, 2022; Sousa et al., 2022). Consequently, it remains unclear how the stability of emulsions is affected when they are formed and flowed through the pore spaces of reservoir under specific conditions.

The presence of colloidal asphaltene in crude oil, as well as high shear, are required for emulsification of the crude oil and water phases during reservoir (Kharrat et al., 2022; Shahsavar et al., 2020; Fani et al., 2022; Wang et al., 2023). There are two contrasting viewpoints regarding the impact of crude oil emulsification on production. The first suggests that emulsification is beneficial, supported by mechanisms such as decreased viscosity, carry-over effects, and improved sweep efficiency (Mariyate and Bera, 2022; Li et al., 2022; Hu et al., 2022; Papadimitriou and Stephanou, 2022; Liu et al., 2022b). Photolithographic glass plate modeling has demonstrated that during the pore transport of oil-in-water emulsions, oil droplets tend to clog at the throat, leading to a change of fluid direction and an increase in swept efficiency (Liu J.B. et al., 2023a, 2023c; Liu et al., 2023d). Observing the blocking and regulatory effects of water-in-oil emulsions can be challenging due to the color of the crude oil. Some researchers have successfully utilized microemulsions for oil recovery, which typically necessitate much higher injection pressures than pure water phases (Ding et al., 2022). Further studies revealed that when water content at the production end exceeds 98%, the addition of surfactants and continuation of the water flooding can result in higher water-phase drive pressures than the initial drive, ultimately enhancing recovery rates (Tian et al., 2023; Sun et al., 2016). This underscores the role of crude oil emulsification, following the blockage of favorable flow paths, in enhancing oil recovery. Moreover, the emulsioncarrying action extends beyond conventional reservoirs. Following hydraulic fracture modification in tight reservoirs, methods like soaking were employed to enhance oil recovery, still relying on the emulsion-carrying mechanism (Liu et al., 2020; Zhao et al., 2022; Zhang et al., 2022; Meng et al., 2023b). Conversely, there is a viewpoint suggesting that crude oil emulsification may adversely affect well production. The general consensus is that emulsifying crude oil into water-in-oil emulsions increases viscosity and the liquid resistance effect, potentially leading to reservoir blockages (Liu et al., 2023e; Liang et al., 2017; Mohammadzadeh Shirazi et al., 2019; Foxenberg et al., 1996; Zhong et al., 2022). In cases where low-temperature multi-thermal fluid throughput is injected into thick oil wells, as seen in the Nanbu 35-2 Oil Field in the Bohai Sea, severe emulsion blockages can lead to dramatic reductions in production capacity and even halt production. Experimental research has shown that permeability can decrease by up to 99% when heavy oil forms a stable water-in-oil

emulsion within the core, effectively blocking the flow channel (Yu et al., 2017).

The dispersed phase droplet size and distribution, as well as the viscosity of the continuous phase, determine the emulsion seepage resistance. This influence is caused by the interaction between the dispersed phase and the continuous phase, the deformation of the dispersed phase, and the interaction of droplets (Trallero, 1995; Plasencia et al., 2013). Mohamed and Saleh (2009) carried out flow experiments using sand-filled tubes to simulate the alkali drive process in heavy oil reservoirs. The experimental findings indicated that after a period of water flooding, injecting a suitable volume of alkali solution into the tube, which was saturated with crude oil, led to the formation of a water-in-oil emulsion within the pore space and an increase in injection pressure. Regina (2006) found that water-in-oil emulsions can block high-permeability channels, resulting in increased injection pressure. The plugging effect of an emulsion is influenced by the depth of its penetration and the permeability of the core. Deeper emulsion penetration and lower core permeability enhance the visibility of the plugging effect (Zeidani et al., 2008). Mars et al. (2011) performed capillary experiments and then discovered that water-in-oil emulsion droplets are dynamically clogged at the throat, primarily influenced by the friction between droplets and the extent of droplet variation caused by changes in injection pressures. When water-in-oil emulsions flow through porous media, the dispersed phase clogs the pores, increasing injection pressures and therefore expanding the sweep efficiency. However, crude oil is easily emulsified in porous media, which may cause blocking issues in the reservoir. There have been no parameters produced to characterize the degree of blocking in water-in-oil emulsions, and the factors controlling this are still unknown.

This study focuses on the Bohai Oil Field, employing laboratory-based experimental methods to investigate the flow behavior of water-in-oil emulsions within porous media. The study specifically examines how emulsion water content, core permeability, and flow rate influence seepage resistance. The overarching objective of the study is to explain the factors that influence the flowability of water-in-oil emulsions in reservoirs.

2. Experimental

2.1. Materials

The experimental cores used are cylindrical artificial cores (25 mm \times 50 mm) with gas permeabilities of 50, 100, and 300 mD, respectively. The crude oil comes from a certain oilfield in the Bohai Sea, with a viscosity of 8.09 mPa \cdot s at 60 °C and a density of 860 mg/L. According to the actual conditions of the oilfield water, the synthetic brine salinity is 10,000 mg/L. The chemicals used to prepare the synthetic brine are all Aladdin reagents and include magnesium sulfate (MgSO₄), sodium chloride (NaCl), and sodium bicarbonate (NaHCO₃).

2.2. Determination of crude oil components

The dehydration of crude oil is subjected to component analysis using a TLC/FID instrument. A certain amount of sample was taken and mixed with chloroform to prepare a 60 mL/L solution. This solution was then applied to a thin-layer plate and exposed to a series of solvent systems to separate saturated hydrocarbons, aromatic hydrocarbons, resins, and asphaltenes, respectively. Quantification of the components of crude oil could be achieved using the area method and the calibration normalization method.

2.3. Interfacial tension measurement

Crude oil was dehydrated through electric heating. Subsequently, the interfacial tension between the crude oil and the synthetic brine was tested using a rotary interfacial tensiometer (SVT20) at various temperatures of 30, 40, 50, 60, and 70 $^{\circ}$ C. The experiment was carried out at a speed of 6000 rpm.

2.4. Preparation and characterization of emulsion

Emulsification experiments were performed using dehydrated crude oil and synthetic brine at different rotational rate and water content levels. The experiments were performed at rotational rates of 2000, 3000, and 4000 rpm for 50 min at 60 °C, and the water content levels tested were 20%, 40%, and 60% by weight, respectively. To achieve thorough emulsification of oil and water, the water phase was gradually added dropwise into the crude oil during the emulsification process. The emulsion droplet size and morphology were observed using a microscope (Pro580ES), and ImageJ was used to measure and statistically analyze the emulsion droplet size. A rheometer (HAKE) was used to measure the viscosity changes of the emulsion at different temperatures, namely 50, 60, and 70 °C, with a shear rate of 10 s $^{-1}$.

2.5. Microporosity analysis of the rock cores

The initial step involved sampling artificial cores with a volume of approximately 2 cm³, followed by a gold-spraying process to enhance the electrical conductivity. Subsequently, an electron microscope (Hitachi 2000) was used to examine the microscopic pore structure. Meanwhile, nuclear magnetic resonance technology (MicroMR, Suzhon) was used to measure the size and distribution of core pores (Zhang et al., 2023; Meng et al., 2023a).

2.6. Water-in-oil emulsion injection experiment

The cores were first dried at $105\,^{\circ}\text{C}$ for $48\,\text{h}$, then vacuumed and saturated with crude oil. The crude oil was injected at a rate of 0.01, 0.03, and 0.05 mL/min into the core until the injection pressures stabilized, respectively. Then, emulsions with varied water content (10%, 20%, 30%, 40%, and 50%) were prepared according to Section 2.4. The emulsion viscosity was tested by a rheometer at 50, 60, and 70 °C. The emulsions were observed microscopically with a microscope. The emulsions were injected at a rate of 0.01, 0.03, and 0.05 mL/min into the core until the injection pressures stabilized, respectively. The emulsion injection experiments typically last between 6 and 8 h, with pressure stabilization occurring within 30–40 min. The schematic diagram of the experimental setup is shown in Fig. 1.

3. Results and discussion

3.1. Crude oil component analysis

Resins and asphaltenes present in crude oil act as natural emulsifiers due to their amphiphilic nature, meaning they have both hydrophilic and hydrophobic components. This characteristic enables them to adsorb effectively at the oil—water interface, substantially reducing interfacial free energy and thereby decreasing the interfacial tension between oil and water. As depicted in Fig. 2, distinct peak areas correspond to the components contained in the crude oil. The results show that the crude oil comprises approximately 3.01% asphaltenes, 17.24% saturates, 16.72% resins, and 63.03% aromatics. The high content of resin and asphaltene fractions in the crude oil enhanced its ability to emulsify.

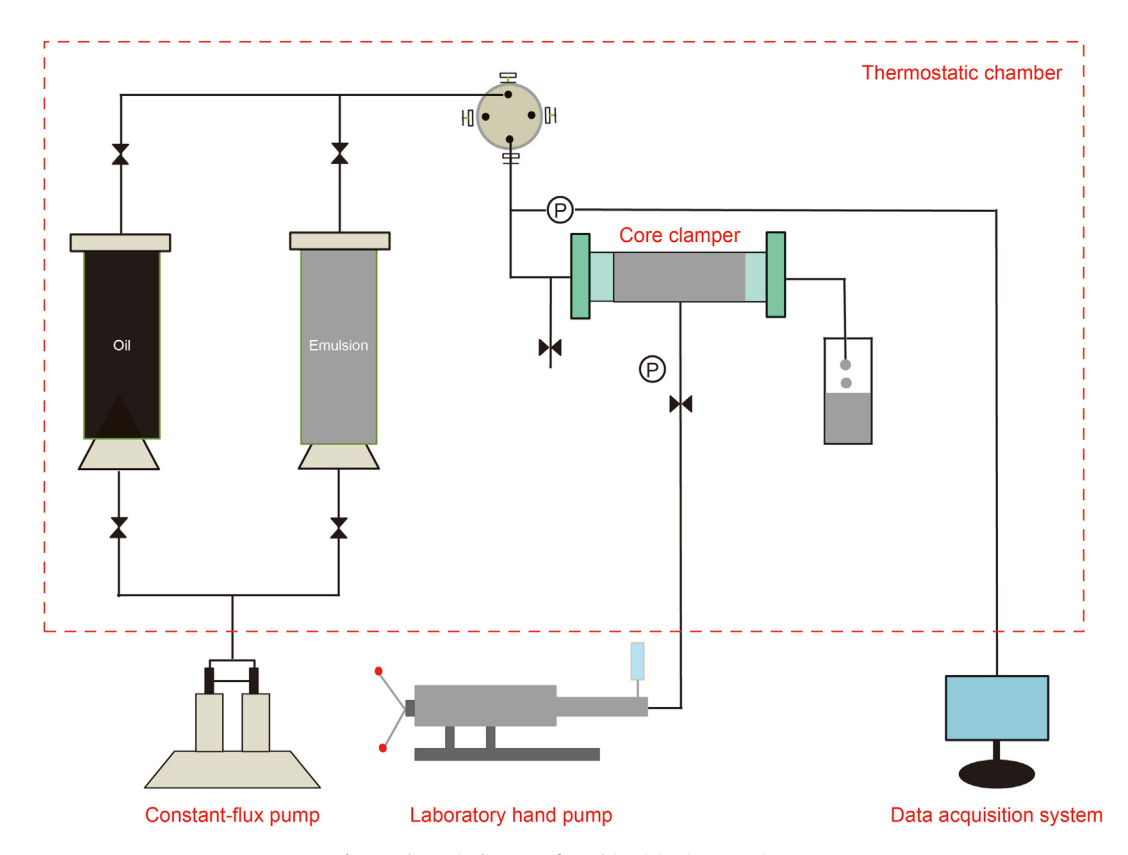


Fig. 1. Schematic diagram of emulsion injection experiment.

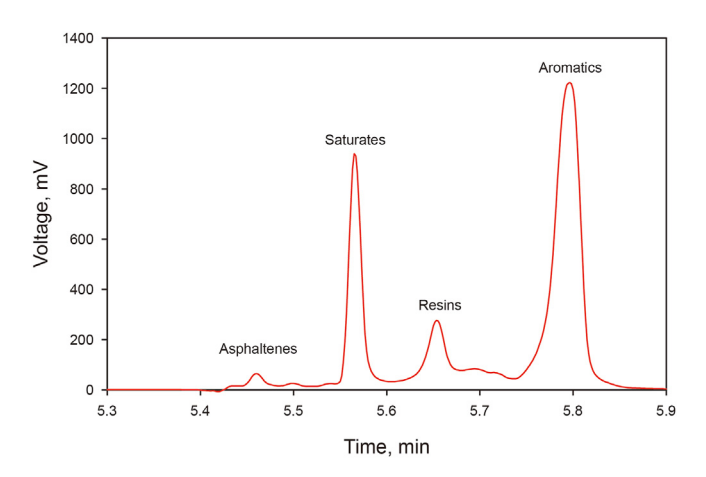


Fig. 2. Chromatogram of crude oil components.

3.2. Interfacial tension

The interfacial tension between the crude oil and the synthetic brine is illustrated in Fig. 3. At room temperature (30 °C), the interfacial tension was 4 mN/m, whereas at the reservoir temperature (60 °C), it was 2.67 mN/m. Notably, the interfacial tension between oil and water exhibited relatively minor fluctuations with temperature changes.

3.3. Emulsion viscosity and droplet size distribution

The crude oil was settled for 15 days, after which the upper layer

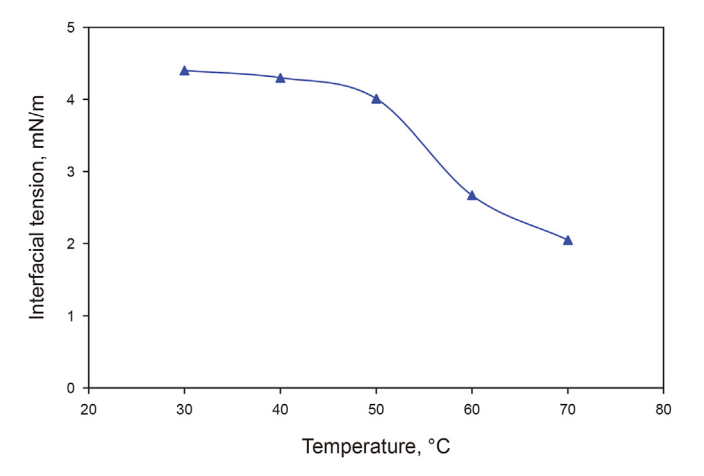


Fig. 3. Interfacial tension between crude oil and synthetic brine.

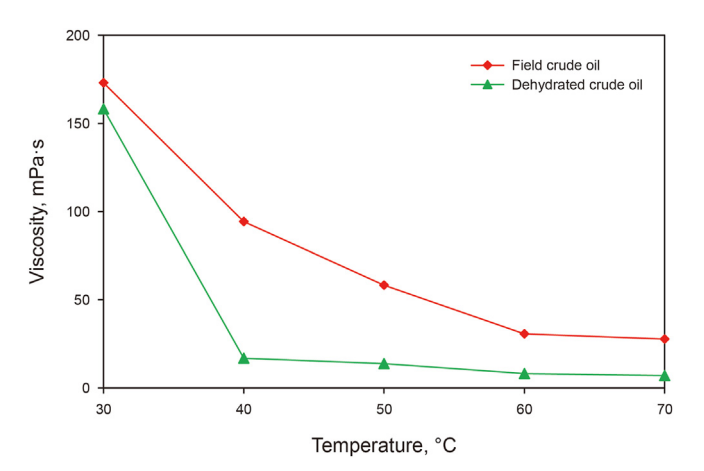


Fig. 5. Changes in the viscosity of crude oil before and after dehydration.

was removed for further rheological and microscopic analyses. The emulsion droplets range from 2 to 4 μm and contain substantial amounts of colloids and asphaltenes, as illustrated in Fig. 4. The viscosity—temperature curve shown in Fig. 5 demonstrates variations in the viscosity of the crude oil before and after dehydration. Initially, at the reservoir temperature of 60 °C, the undehydrated crude oil had a viscosity of 30 mPa·s. However, after dehydration of crude oil, the viscosity under the same conditions decreased to 8.09 mPa·s. The viscosity of a water-in-oil emulsion is primarily determined by internal friction in the oil phase as well as internal friction between the water and oil phases. Crude oil viscosity only reflects the internal friction of the oil phase.

3.3.1. Effect of rotational rate

The viscosity of water-in-oil emulsions shows a positive correlation with rotational rate. Results showed that an increase in the viscosity of the emulsion was attained via increasing the rotational rate. For example, at 60 °C and 60% water content, the emulsion viscosity increased from 81.81 to 91.31 mPa·s as the rotational rate increased from 2000 to 4000 rpm, as shown in Fig. 6. At a steady water content, an increased rotational rate leads to smaller droplet sizes and an increase in the dispersed surface area of the aqueous phase in the oil phase, resulting in increased internal friction between the oil and water phases.

3.3.2. Effect of water content

The viscosity of water-in-oil emulsions is positively correlated with water content, demonstrating that an increase in water content typically leads to an increase in emulsion viscosity. At 60 °C, the viscosity of the dehydrated crude oil was 13.2 mPa·s, but with a

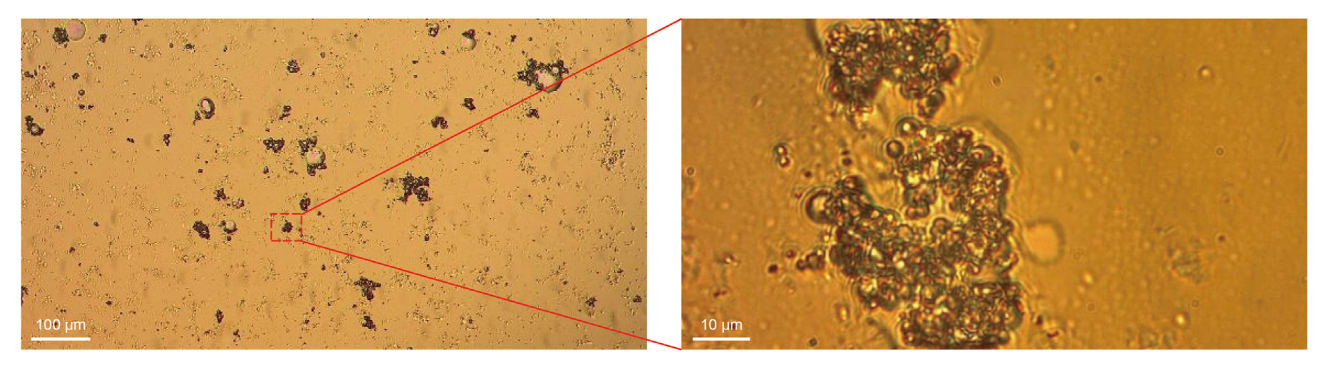


Fig. 4. Photo of undehydrated crude oil by microscope.

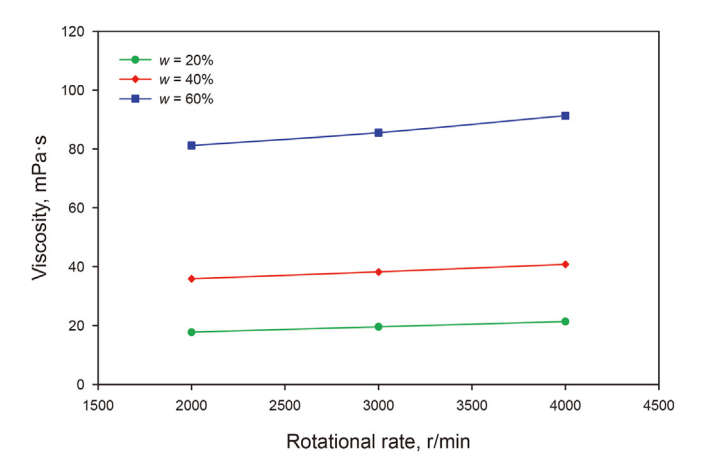


Fig. 6. Changes in the viscosity of water-in-oil emulsions with rotational rate (60 $^{\circ}$ C) (w is the water content).

water content increase to 50%, the emulsion viscosity surged to $63.14 \text{ mPa}\cdot\text{s}$, as depicted in Fig. 7.

3.3.3. Emulsion droplet size distribution

Under consistent experimental conditions, as illustrated in Fig. 8, the size and amount of emulsion droplets increased with increasing water content in the emulsion. Specifically, at a water content of 10%, the majority of emulsion droplets were sized between 0 and 3 μm . However, as the water content increased to 30%, the dominant emulsion droplet size ranged from 3 to 4 μm , accompanied by the appearance of larger droplets exceeding 10 μm . When the water content reached 50%, there was a significant increase in the proportion of emulsion droplets exceeding 10 μm in size.

3.4. Microporosity of the rock cores

The alignment of the core pore diameters with the emulsion droplet size significantly influences the flow behavior of the emulsion within the core pore space. The influence of core permeability on pore size distribution was investigated using

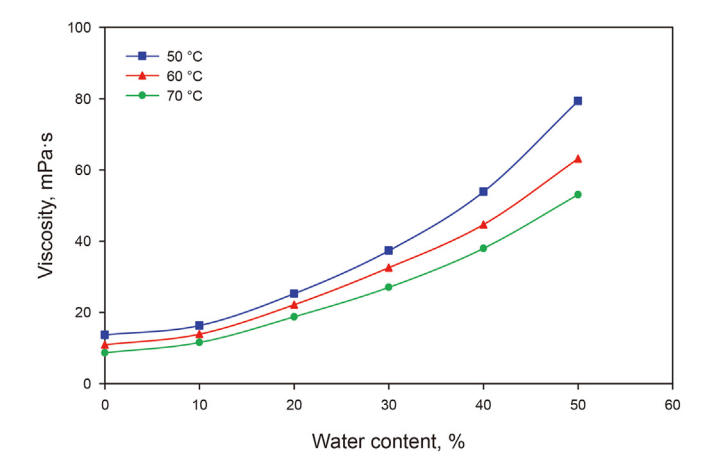


Fig. 7. Changes in the viscosity of water-in-oil emulsions under different water content (rotational rate of 5000 r/min).

electron microscope scanning and nuclear magnetic resonance techniques. As shown in Fig. 9, when the core permeability was 50 mD, the predominant pore diameters were distributed in the range from 2 to 4 μ m, with a smaller portion of pores measuring less than 1 μ m. Upon increasing the core permeability to 100 mD, the dominant pore diameters range from 3 to 7 μ m. Subsequently, when the core permeability was increased to 300 mD, the primary distribution of pore diameters expanded to within the range of 8–19 μ m.

3.5. The characteristics of emulsions flowing in porous media

When crude oil flows in a porous medium, flow resistance is primarily governed by the magnitude of internal friction within the oil itself and the friction between the oil phase and the pore walls. However, emulsion viscosity changes and liquid resistance effects synergistically affect the flow resistance of water-in-oil emulsions as they flow through porous media.

3.5.1. Core permeability effects

The permeabilities of the experimental cores were 50, 100, and 300 mD, and the flow rate was set at 0.05 mL/min. The theoretical injection pressure, derived from Darcy's law, was utilized to assess the impact of emulsion viscosity on flow resistance. Practically, the actual injection pressure is affected by both the viscosity of the emulsion and the liquid resistance effect. This approach allows for the quantification of how the liquid resistance effect and emulsion viscosity contribute to the flow resistance of emulsions in porous media. The comparison between actual injection pressures and theoretical injection pressures is detailed in Fig. 10, illustrating the interplay of viscous forces and the liquid resistance effect when water-in-oil emulsions flow through cores. For instance, when the core permeability was 50 mD, the actual injection pressure followed a power exponential growth pattern as the water content in the emulsion increased. In such cases, the actual injection pressure could reach up to 13 MPa, with the liquid resistance effect playing a dominant role in the overall flow resistance. When the water content was maintained below 30% and the core permeability was 100 mD, the actual injection pressure was up to 0.526 MPa. However, as the water content exceeded 30%, there was a notable increase in actual injection pressure to 11.3 MPa, mainly due to the liquid resistance. In situations where the water content was under 30% and the core permeability was 300 mD, the actual injection pressure increased as the water content increased. Conversely, when the water content exceeded 30%, the actual injection pressure decreased as the water content increased.

As illustrated in Fig. 11, when the core permeability is 50 mD and the core throat diameter is small, the impact of crude oil viscosity on flow resistance ranges from 2.5% to 11.4%. When the core permeability was 100 mD, this influence ranged from 1.3% to 22% as the throat diameter increased. At a core permeability of 300 mD, the effect of crude oil viscosity on flow resistance escalates from 13.9% to 68%. When emulsions flow through porous media, the interplay between crude oil viscosity and the liquid resistance effect crucially affects the emulsions flow capacity. When the ratio of emulsion droplet size to throat diameter is large, the liquid resistance effect dominates. Conversely, when the ratio is small, the viscosity of the crude oil takes precedence. It is important to note that the water content of the emulsion primarily influences the size and number of droplets, thereby significantly affecting the emulsion viscosity.

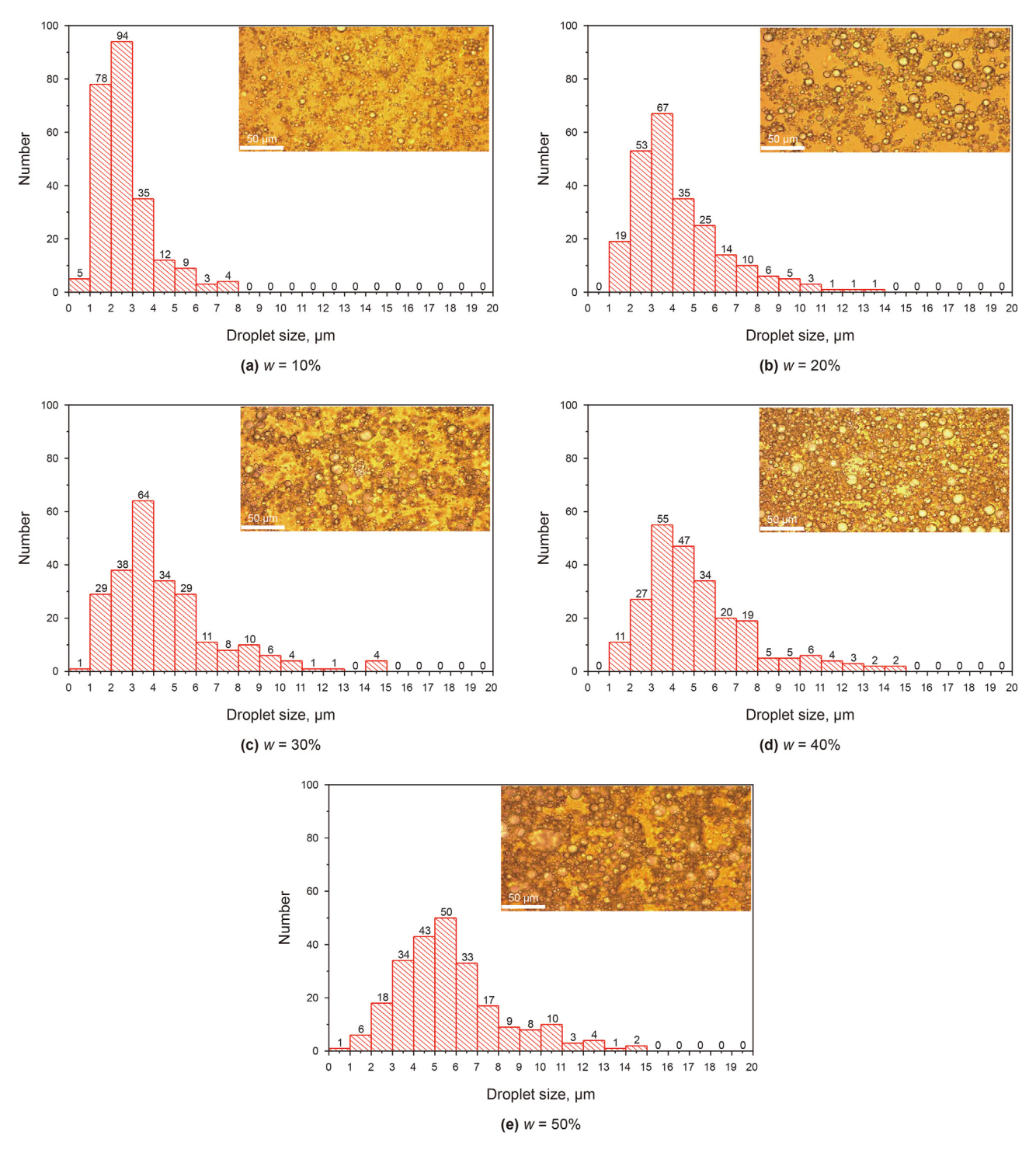


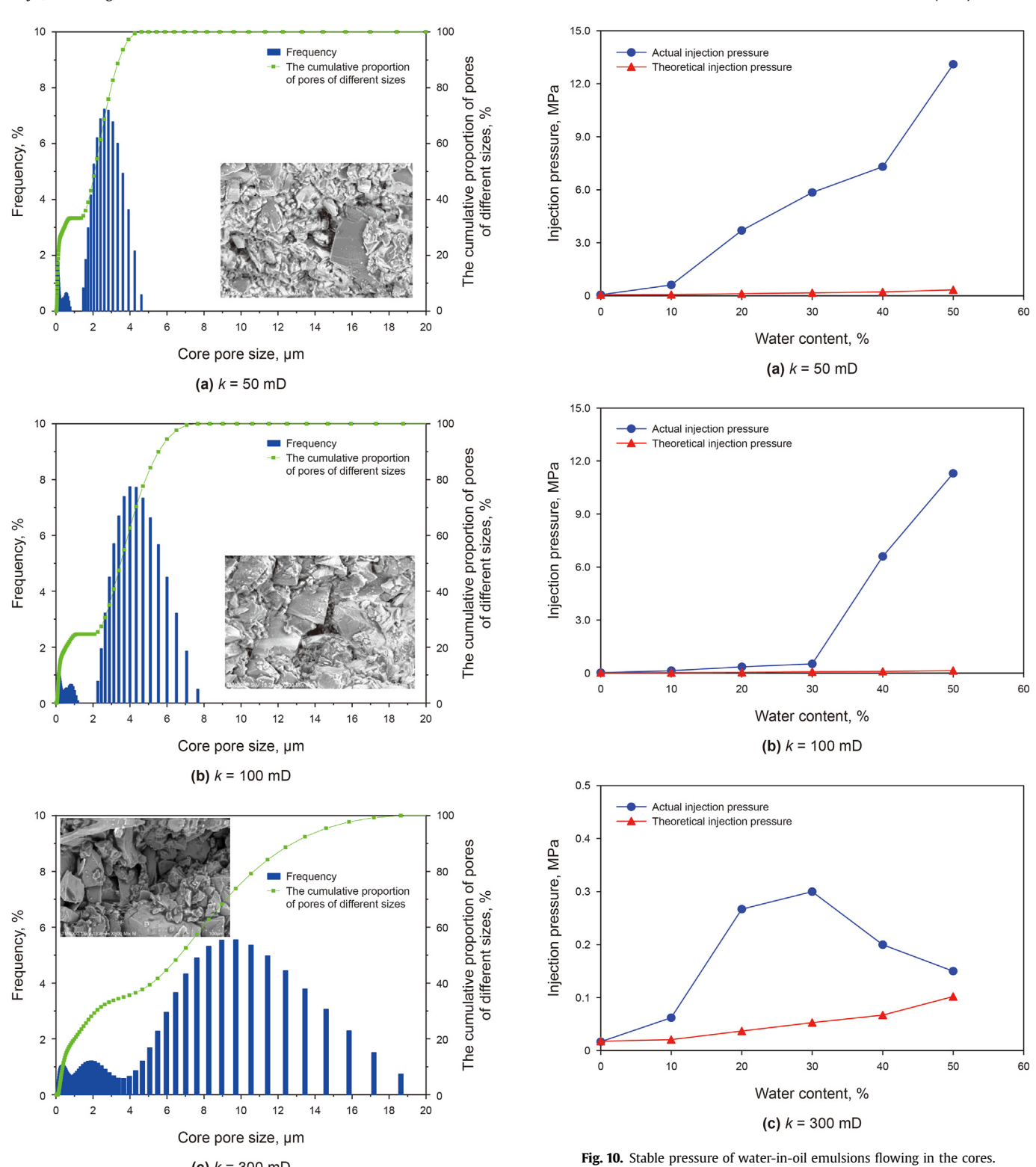
Fig. 8. Droplet size distributions of water-in-oil emulsions with different water content.

3.5.2. Effect of flow rate

The emulsions were injected at a rate of 0.01, 0.03, and 0.05 mL/min into the core with permeability of 100 mD. As shown in Fig. 12, the injection pressure increased as the flow rate increased. When the water content of the emulsion was below 30%, the impact of the flow rate on injection pressure was relatively minimal. However, once the water content exceeded 30%, the effect of the liquid resistance effect became more significant, and the influence of flow rate on injection pressure notably increased.

3.5.3. The threshold pressure gradient

When the seepage velocity maintains a linear relationship with the pressure gradient, the flow adheres to Darcy's law, which is primarily governed by viscous resistance. However, deviations from this linear relationship occur when seepage velocities become extremely high or low, rendering Darcy's law inapplicable. At high seepage velocities, significant inertial forces emerge, and experimental data show that the pressure gradient becomes proportional to the square of the seepage velocity. At lower velocities, as fluids flow through porous media, they encounter additional resistance



(c) k = 300 mD

due to physicochemical interactions at the pore surfaces of the rock, which is particularly notable when external forces are minimal. Resins and asphaltenes in crude oil can adsorb onto the rock surface, leading to substantial viscous resistance. The water phase interacts with the clay to form a hydration film, resulting in the formation of bound water on the rock surface. The bound water also

Fig. 9. Pore distribution of cores.

contributes to the additional resistance during seepage. Furthermore, when surfactants are abundant, crude oil can easily emulsify within the pore space and be flowed as an emulsion. When flowing through the pore throat or constricted channels, this leads to a liquid resistance effect, resulting in significant additional resistance. Fig. 13 illustrates the initiation pressures under different conditions: (a) the threshold pressure at which the fluid flows through the pore of least resistance; (b) the threshold pressure at

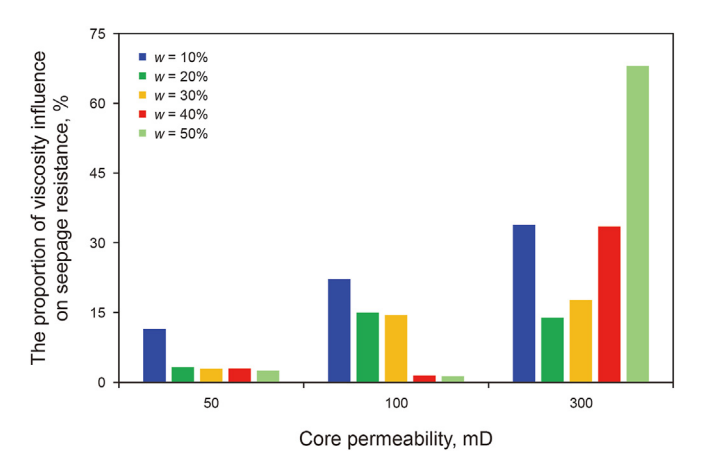


Fig. 11. Percentage of the effect of emulsion viscosity on flow resistance.

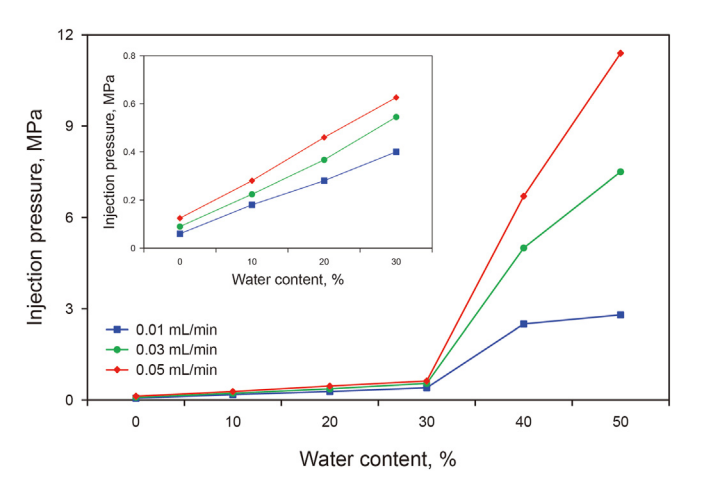


Fig. 12. Injection pressure at different flow rates (k = 100 mD).

which the fluid flows through the pore of greatest resistance; and (c) represents the intersection of the reverse extension of the straight-line segment "d-e" with the vertical coordinate, indicating the threshold pressure gradient.

Fig. 14 demonstrates that the threshold pressure gradient has a linear negative correlation with core permeability. Specifically, when the core permeability was 100 mD, the threshold pressure

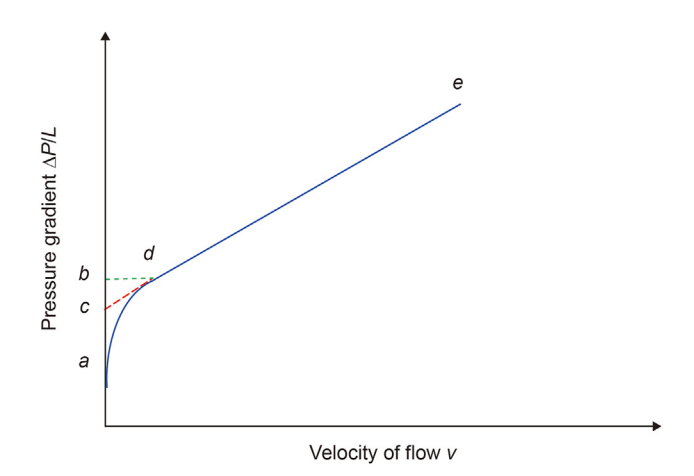


Fig. 13. The threshold pressure gradient diagram.

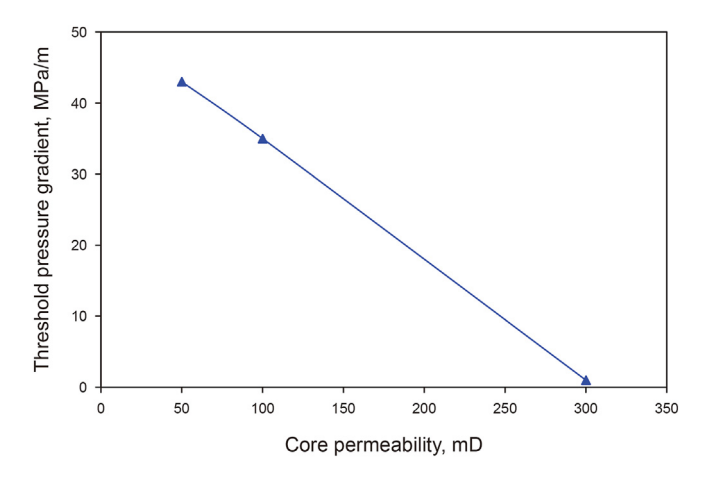


Fig. 14. The threshold pressure gradient of cores with different permeabilities (w=50%).

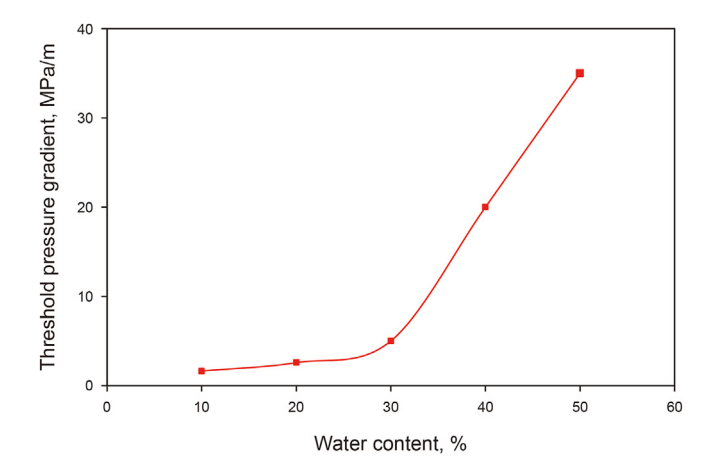


Fig. 15. The threshold pressure gradient of the emulsion with different water content (k=100~mD).

gradient was recorded at 35 MPa/m and decreased to 1 MPa/m as the core permeability increased to 300 mD. It was crucial to note that in medium permeability and low permeability reservoirs, water-in-oil emulsion could lead to reservoir blocking.

The relationship between the emulsion water content and the threshold pressure gradient adheres to a power-function pattern.

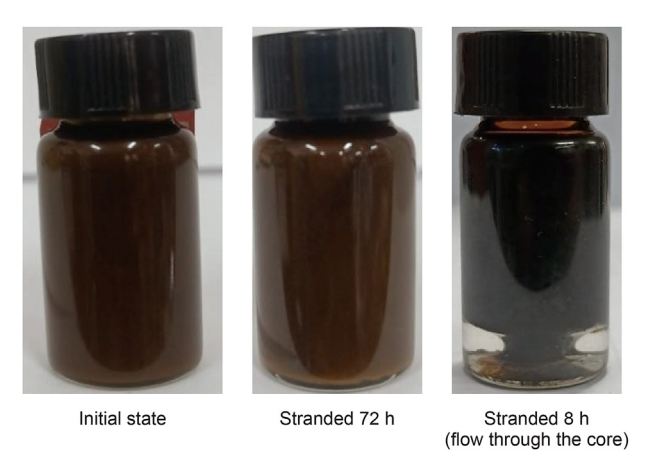
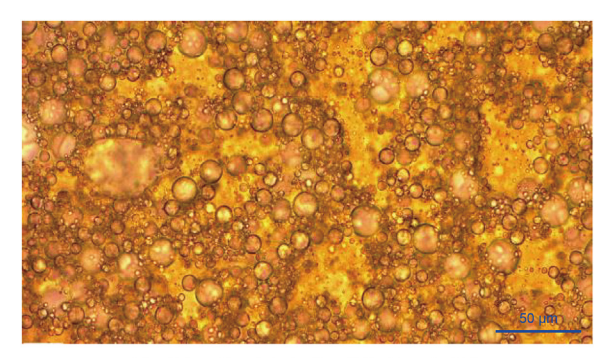
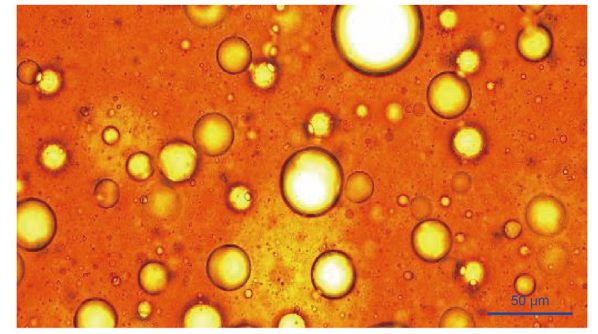


Fig. 16. Emulsion stability under different conditions (w = 50%).





Emulsion droplets before injection (0 PV)

Emulsion droplets after injection (2.0 PV)

Fig. 17. Microscopy images of water-in-oil emulsion at various injection volumes (k = 100 mD, w = 50%).

The threshold pressure gradient increased with the emulsion water content. Fig. 15 reveals that with an emulsion water content below 30%, the starting pressure gradient ranged from 1.63 to 5.01 MPa/m. When the water content exceeded 30%, the threshold pressure gradient increased markedly.

Fig. 16 shows no water was separated at the bottom after the water-in-oil emulsion settled in a volumetric flask at 60 °C for 72 h, indicating that the emulsion remained stable and did not demulsify during this time. However, when the same emulsion was flowed through the core with permeability of 100, the emulsion began to demulsify. The experiment demonstrated that the stability of water-in-oil emulsions decreased after experiencing the shearing forces within throats.

Micrographs of the emulsion, presented in Fig. 17, revealed that when the water-in-oil emulsion flows through the throat, water droplets clog and adhere to each other in the pores. Initially, at 0 pore volume (PV), many small emulsion droplets were visible. However, as the injection volume reached 2 PV, there was a noticeable increase in emulsion droplet size, despite the number of water droplets remaining lower than that at 0 PV. Furthermore, viscosity testing confirmed that the viscosity of the produced fluids was positively correlated with the injection volume. In other words, the emulsion viscosity tended to increase as the injection volume increased, as shown in Fig. 18. Due to the liquid resistance effect, the emulsion viscosity remained lower than at 0 PV, even when the injection volume reached 2 PV.

As illustrated in Fig. 19, after the water droplets are clogged in the throat, they begin to coalesce and aggregate in the larger pore

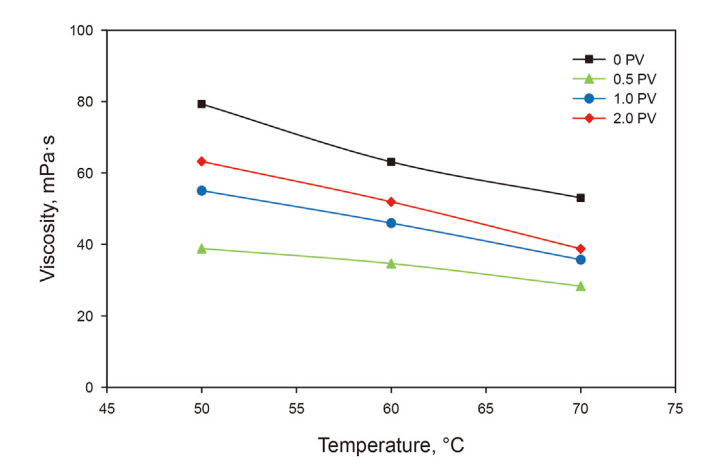
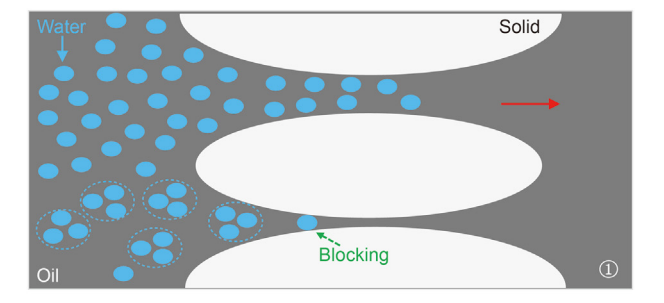
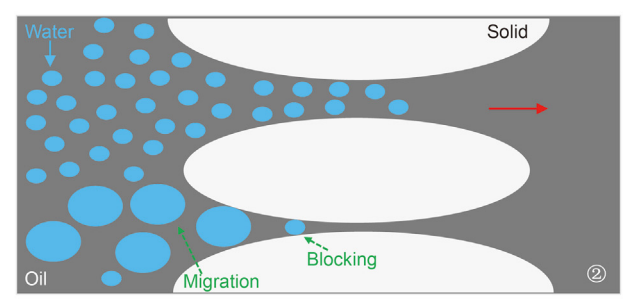


Fig. 18. Changes of viscosity of the produced fluids (emulsion) at different injection volumes (w = 50%).





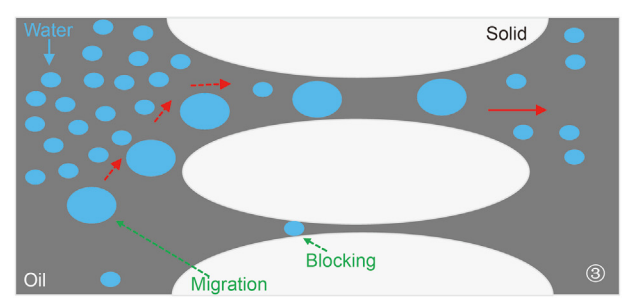


Fig. 19. The process of water-in-oil emulsion flowing through pore-throat channel.

spaces. These larger water droplets can then overcome the liquid resistance effect and flow through the throat as the injection pressure increases.

In summary, a higher content of resins and asphaltenes in crude oil reduced the oil—water interfacial tension, which enhanced the emulsification of crude oil and sustained its stability. Shear rate and water content affect emulsion viscosity mainly by influencing the size and number of emulsion droplets. The liquid resistance effect plays a crucial role in the flow of water-in-oil emulsions in porous media. When the size of emulsion droplets was larger than that of throats, the liquid resistance effect had a greater impact on the seepage resistance, and when the size of emulsion droplets was

smaller than that of throats, the emulsion viscosity had a more pronounced impact on the seepage resistance. Due to the liquid resistance effect, the size of emulsion droplets increased upon flow through porous media, thereby reducing emulsion stability.

4. Conclusions

In order to clarify the emulsification problem of crude oil in the Bohai Oilfield, this paper focused on the characteristics of water-inoil emulsion as well as the liquid resistance effect by using laboratory experiments. The specific conclusions are as follows.

- (1) The viscosity of the water-in-oil emulsion was positively correlated with the shear rate and water content. As the shear rate and water content increased, the emulsion viscosity also increased. The size and number of water droplets in the emulsion played a significant role in determining the internal friction between water and crude oil. Consequently, the water-in-oil emulsion viscosity increased with an increase in the total surface area of the water phase within the crude oil.
- (2) The emulsion viscosity and the liquid resistance effect influence the seepage resistance of emulsions in porous media. The match between the emulsion droplet size and the core throat plays a crucial role in determining the seepage resistance. When the size of majority of emulsion droplets exceeds the throat diameter, the liquid resistance effect constitutes over 90% of the total seepage resistance. Conversely, when the size of most emulsion droplets is smaller than the throat diameter, the emulsion viscosity contributed to more than 60% of the increase in seepage resistance.
- (3) A threshold pressure gradient is established when a water-in-oil emulsion forms in a reservoir. When the core permeability is low (50–100 mD), this threshold pressure gradient can range from 35 to 43 MPa/m. When the core permeability is 300 mD, the threshold pressure gradient is lowered to 1 MPa/m.
- (4) The stability of the water-in-oil emulsion was reduced after flow through the core. This result is attributed to the fact that the liquid resistance effect caused water droplets to aggregate in the pores to form large-size water droplets when the water-in-oil emulsion flowed through the throat, thereby reducing emulsion stability.

CRediT authorship contribution statement

Lei-Lei Jia: Writing — review & editing, Writing — original draft, Conceptualization. **Li-Guo Zhong:** Writing — review & editing, Conceptualization. **Shi-Hao Li:** Writing — review & editing. **Yu-Hao Liu:** Writing — review & editing. Conceptualization. **Chang-Hao Hu:** Writing — review & editing. **Guo-Dong Wang:** Writing — review & editing. **Yu-Ning Gong:** Writing — review & editing. **Ce Shang:** Writing — review & editing. **Yao-Tu Han:** Writing — review & editing. **Jin Li:** Writing — review & editing.

Declaration of competing interest

The authors declare that they have no known competing financial interests or personal relationships that could have appeared to influence the work reported in this paper.

Acknowledgments

This study is financially supported by the National Natural Science Foundation of China (No. ZX20230212).

References

- Abdullah, M.M.S., Al-Lohedan, H.A., 2022. Alginate-based poly ionic liquids for the efficient demulsification of water in heavy crude oil emulsions. Fuel 320, 123949. https://doi.org/10.1016/j.fuel.2022.123949.
- Adil, M., Onaizi, S.A., 2022. Pickering nanoemulsions and their mechanisms in enhancing oil recovery: a comprehensive review. Fuel 319, 123667. https:// doi.org/10.1016/j.fuel.2022.123667.
- Cao, C.X., Gu, S.H., Song, Z.J., Xie, Z.H., Chang, X.Y., Shen, P.P., 2022. The viscosifying behavior of W/O emulsion and its underlying mechanisms: considering the interfacial adsorption of heavy components. Colloid. Surface. 632, 127794. https://doi.org/10.1016/j.colsurfa.2021.127794.
- Chen, C., Jing, Z.F., Feng, C., Feng, C., Zou, X., Qiao, M., Xu, D., Wang, S., 2023. Two-phase flow and morphology of the gas—liquid interface for bubbles or droplets in different microchannels. Phys. Fluids 35, 091302. https://doi.org/10.1063/5.0157473.
- Ding, B.X., Dong, M.Z., Chen, Z.G., Kantzas, A., 2022. Enhanced oil recovery by emulsion injection in heterogeneous heavy oil reservoirs: experiments, modeling and reservoir simulation. J. Pet. Sci. Eng. 209, 109882. https://doi.org/10.1016/j.petrol.2021.109882.
- Dong, B., Qin, Z.Y., Wang, Y.W., Zhang, J.H., Xu, Z., Liu, A.X., Guo, X.Q., 2022. Investigating the rheology and stability of heavy crude oil-in-water emulsions using APG08 emulsifiers. ACS Omega 7, 37736–37747. https://doi.org/10.1021/acsomega.2c04684.
- Fani, M., Pourafshary, P., Mostaghimi, P., Mosavat, N., 2022. Application of micro-fluidics in chemical enhanced oil recovery: a review. Fuel 315, 123225. https://doi.org/10.1016/i.fuel.2022.123225.
- Foxenberg, W.E., Ali, S.A., Ke, M., 1996. Effects of completion fluid loss on well productivity. In: SPE Formation Damage Control Symposium. https://doi.org/ 10.2118/31137-MS.
- Gong, J.C., Ji, Y.F., Wang, Y.L., Fan, H.M., Wei, Z.Y., Li, C.Y., 2022. Preparation and interfacial behavior of surface-active microspheres for both emulsion stabilization and profile control. J. Pet. Sci. Eng. 208, 109414. https://doi.org/10.1016/ i.petrol.2021.109414.
- Gu, Z.H., Li, Z.M., Xu, Z.X., Zhang, C., 2022. Microscopic mechanical model analysis and visualization investigation of SiO₂ nanoparticle/HPAM polymer foam liquid film displacing heavy oil. Langmuir 38, 9166–9185. https://doi.org/10.1021/acs.langmuir.2c00817.
- Hu, J.J., Zhang, G.C., Jiang, P., Ge, J.J., Pei, H.H., Wang, X., 2022. Study on the chemical structure characterization and emulsification-stripping of heavy oil. J. Pet. Sci. Eng. 215, 110592. https://doi.org/10.1016/j.petrol.2022.110592.
- Kharrat, A., Brandstätter, B., Borji, M., Ritter, R., Arnold, P., Fritz-Popovski, G., Paris, O., Ott, H., 2022. Development of foam-like emulsion phases in porous media flow. J. Colloid Interface Sci. 608, 1064–1073. https://doi.org/10.1016/j.jcis.2021.10.022.
- Li, X.X., Yue, X.A., Zou, J.R., Yan, R.J., 2022. Effect of in-situ emulsification of surfactant on the enhanced oil recovery in low-permeability reservoirs. Colloid. Surface. 634, 127991. https://doi.org/10.1016/j.colsurfa.2021.127991.
- Li, Z., Fuentes, J., Chakraborty, A., Zamora, E., Prasad, V., Vázquez, F., Xu, Z.H., Liu, Q.X. César, Flores, McCaffrey, W.C., 2023. Dehydration of water-in-crude oil emulsions using polymeric demulsifiers: a model for water removal based on the viscoelastic properties of the oil—water interfacial film. Fuel 332, 126185. https://doi.org/10.1016/i.fuel.2022.126185.
- Liang, T.B., Gu, F.Y., Yao, E.D., Zhang, L.F., Yang, K., Liu, G.H., Zhou, F.J., 2017. Formation damage due to drilling and fracturing fluids and its Solution for tight naturally fractured sandstone reservoirs. Geofluids, 9350967. https://doi.org/10.1155/2017/9350967
- Liu, J.B., Zhong, L.G., Hao, T.C., Ren, L., Liu, Y.G., 2022a. A collaborative emulsification system capable of forming stable small droplets of oil-in-water emulsions for enhancing heavy oil recovery. J. Mol. Liq. 355, 118970. https://doi.org/10.1016/i.mollig.2022.118970.
- Liu, J.B., Liu, S., He, Y.X., Zhong, L.G., Hao, T.C., Liu, Y.G., Wang, P., Gao, P.C., Guo, Q.H., 2022b. Experimental study of produced fluid emulsification during water/ steam flooding for heavy oil recovery. Energy Fuels. 37, 4308–4319. https:// doi.org/10.1021/acs.energyfuels.2c03211.
- Liu, J.B., Liu, S., Zhang, W., Zhong, L.G., Hao, Y., Zhang, Y.J., Cai, W.B., Du, H.Y., 2023a. Influence of emulsification characteristics on the pressure dynamics during chemical flooding for oil recovery. Energy Fuels 37, 4308–4319. https://doi.org/ 10.1021/acs.energyfuels.2c04010.
- Liu, J.B., Liu, S., Zhong, L.G., Li, Z.L., Zhang, Y.L., Du, H.Y., 2023b. Porous media flooding mechanism of nanoparticle-enhanced emulsification system. Phys. Fluids 35, 033304. https://doi.org/10.1063/5.0141815.
- Liu, J.B., Liu, S., Zhong, L.G., Wang, P., Cao, P.C., Guo, Q.H., 2023c. Ultra-low interfacial tension anionic/cationic surfactants system with excellent emulsification ability for enhanced oil recovery. J. Mol. Liq. 382, 121898. https://doi.org/10.1016/ j.molliq.2023.121989.
- Liu, J.R., Shenga, J.J., Tu, J.W., 2020. Effect of spontaneous emulsification on oil recovery in tight oil-wet reservoirs. Fuel 279, 118456. https://doi.org/10.1016/

j.fuel.2020.118456.

- Liu, S., Zhang, Y.L., Du, H.Y., Liu, J.B., Zhou, Z.X., Wang, Z.Z., Hang, K., Pan, B.S., 2023d. Experimental study on fluid flow behaviors of waterflooding fractured-vuggy oil reservoir using two-dimensional visual model. Phys. Fluids 35, 062106. https://doi.org/10.1063/5.0152685.
- Liu, T.J., Xu, D.R., Lian, W., Kang, W.L., Sarsenbekuly, B., 2023e. Optimization of injection parameters of a microemulsion-type oil displacement agent for heavy oil recovery. Phys. Fluids 35, 113102. https://doi.org/10.1063/5.0174514.
- Ma, J., Yao, M.Q., Yang, Y.L., Zhang, X.Y., 2022. Comprehensive review on stability and demulsification of unconventional heavy oil—water emulsions. J. Mol. Liq. 350, 118510. https://doi.org/10.1016/j.molliq.2022.118510.
- Mariyate, J., Bera, A., 2022. A critical review on selection of microemulsions or nanoemulsions for enhanced oil recovery. J. Mol. Liq. 353, 118791. https:// doi.org/10.1016/i.mollig.2022.118791.
- Mars, M.K., Guzel, T.B., Aleksey, G.T., Alfir, T.A., 2011. Non-equilibrium and nonlinear effects in water-in-oil emulsion flows in porous media. Energy Fuels 25, 1173—1181. https://doi.org/10.1021/ef101053k.
- Meng, M., Ge, H., Shen, Y., Ji, W., Li, Z., 2023a. Insight into water occurrence and pore size distribution by nuclear magnetic resonance in marine shale reservoirs, southern China. Energy Fuels 37 (1), 319–327. https://doi.org/10.1021/acs.energyfuels.2c03395.
- Meng, M., Zhang, Y., Yuan, B., Li, Z., Zhang, Y., 2023b. Imbibition behavior of oil-saturated rock: implications for enhanced oil recovery in unconventional reservoirs. Energy Fuels 37 (18), 13759—13768. https://doi.org/10.1021/acs.energyfuels.3c02501.
- Mohamed, A., Saleh, Arhuoma, 2009. Emulsion Flow in Porous Media and its Application in Alkaline Flooding for Heavy Oil Reservoirs. Ph.D. Dissertation. University of Regina.
- Mohammadzadeh Shirazi, M., Ayatollahi, S., Ghotbi, C., 2019. Damage evaluation of acid-oil emulsion and asphaltic sludge formation caused by acidizing of asphaltenic oil reservoir. J. Pet. Sci. Eng. 174, 880–890. https://doi.org/10.1016/ i.petrol.2018.11.051.
- Onaizi, S.A., 2022. Effect of oil/water ratio on rheological behavior, droplet size, zeta potential, long-term stability, and acid-induced demulsification of crude oil/ water nanoemulsions. J. Pet. Sci. Eng. 209, 109857. https://doi.org/10.1016/ j.petrol.2021.109857.
- Papadimitriou, M.K., Stephanou, P.S., 2022. Modeling the rheological behavior of crude oil—water emulsion. Phys. Fluids 34. https://doi.org/10.1063/5.0123274, 113-107.
- Patil, A., Arnesen, K., Holte, A., Farooq, U., Brunsvik, A., Størseth, T., Johansen, S.T., 2021. Crude oil characterization with a new dynamic emulsion stability technique. Fuel 290, 120070. https://doi.org/10.1016/j.fuel.2020.120070.
- Plasencia, J., Petterson, B., Nydal, O.J., 2013. Pipe flow of water-in-crude oil emulsions: effective viscosity, inversion point and droplet size distribution. J. Pet. Sci. Eng. 101, 35–43. https://doi.org/10.1016/j.petrol.2012.11.009.
- Pu, W.F., He, M.M., Yang, X.R., Liu, R., Shen, C., 2022. Experimental study on the key influencing factors of phase inversion and stability of heavy oil emulsion: asphaltene, resin and petroleum acid. Fuel 311, 122631. https://doi.org/10.1016/ j.fuel.2021.122631.
- Regina, S., 2006. Interfacial Phenomena in Enhanced Heavy Oil Recovery by Alkaline Flood. Ph.D. Dissertation. University of Regina.

- Shahsavar, N., Riazi, M., Malayeri, M.R., 2020. Removal of asphaltene deposition in porous media using emulsified solvents—a visual study. J. Pet. Sci. Eng. 191, 107207. https://doi.org/10.1016/j.petrol.2020.107207.
- Sousa, A.M., Pereira, M.J., Matos, H.A., 2022. Oil-in-water and water-in-oil emulsions formation and demulsification. J. Pet. Sci. Eng. 210, 110041. https://doi.org/ 10.1016/j.petrol.2021.110041.
- Sun, M., Mogensen, K., Bennetzen, M., Firoozabadi, A., 2016. Demulsifier in injected water for improved recovery of crudes that form water/oil emulsions. SPE J. 19 (4), 664–672. https://doi.org/10.2118/180914-PA.
- Sun, Z.Q., Pu, W.F., Zhao, R.B., Pang, S.S., 2022. Study on the mechanism of W/O emulsion flooding to enhance oil recovery for heavy oil reservoir. J. Pet. Sci. Eng. 209, 109899. https://doi.org/10.1016/j.petrol.2021.109899.
- Tian, K.P., Pu, W.F., Wang, Q.L., Li, S.Y., Liu, S., Xie, M.K., Wang, Y.B., 2023. Effect of amphiphilic CaCO₃ nanoparticles on the plant surfactant saponin solution on the oil—water interface: a feasibility research of rnhanced oil recovery. Energy Fuels 37 (17), 12854—12864. https://doi.org/10.1021/acs.energyfuels.3c02164.
- Trallero, J.L., 1995. Oil—water Flow Patterns in Horizontal Pipes. Ph.D Dissertation. The University of Tulsa.
- Vladisavljević, G.T., 2015. Structured microparticles with tailored properties produced by membrane emulsification. Adv. Colloid Interfac. 225, 53–87. https://doi.org/10.1016/j.cis.2015.07.013.
- Wang, G.Z., Xia, Q.L., 2009. Natural gas distribution characteristics, main controlling factors of accumulation and exploration direction in Bohai Sea. China Offshore Oil Gas 21 (1). 15–18 (in Chinese).
- Wang, H.Y., Wei, B., Hou, J., Sun, Z.Z., Du, Q.J., Zhou, K., 2023. Investigation of microflow mechanisms and emulsion size distribution in porous media. Phys. Fluids 35, 091302. https://doi.org/10.1063/5.0171494.
- Xue, Y.G., 2018. Understanding and innovation promote new breakthroughs in oil and gas exploration in Bohai Sea area: review of major exploration progress in Bohai Sea area in recent years. China Offshore Oil Gas 30 (2), 1–8 (in Chinese).
- Yu, L., Dong, M.Z., Ding, B.X., Yuan, Y.G., 2017. Emulsification of heavy crude oil in brine and its plugging performance in porous media. Chem. Eng. Sci. 178, 335–347. https://doi.org/10.1016/j.ces.2017.12.043.
- Zeidani, K., Polikar, M., Huang, H., Boyd, J.W., 2008. Application of emulsion blocking mechanism for sealing the near wellbore region. J. Can. Pet. Technol. 47 (5). https://doi.org/10.2118/08-05-40.
- Zhang, F., Jiang, Z.X., Zhang, Y.H., Hu, B., Yang, Z.Q., Yang, Y.H., Tang, X.L., Xiao, H.M., Zhu, L., Han, Y.H., 2023. A new method for converting *T*₂ spectrum into pore radius. J. Earth Sci. 34 (4), 966–974. https://doi.org/10.1007/s12583-021-1576-y.
- Zhang, Y.J., Zou, Y., Zhang, Y., Wang, L.Y., Liu, D.Q., Sun, J., Ge, H.K., Zhou, D.S., 2022. Experimental study on characteristics and mechanisms of matrix pressure transmission near the fracture surface during post-fracturing shut-in in tight oil reservoirs. J. Pet. Sci. Eng. 219, 111133. https://doi.org/10.1016/j.petrol.2022.111133.
- Zhao, M.W., Yan, X.W., Cheng, Y.L., Yan, R.Q., Dai, C.L., 2022. Study on the imbibition performance and mechanism of a fracturing fluid and its gel breaking liquid. Energy Fuels 36, 13028–13036. https://doi.org/10.1021/acs.energyfuels.2c02869.
- Zhong, L.G., Liu, J.B., Yuan, X.N., Wang, C., 2022. Subsurface sludge sequestration in cyclic steam stimulated heavy-oil reservoir in Liaohe Oil Field. SPE J. 25 (3), 1113–1127. https://doi.org/10.2118/195415-PA.